Since January 2020 Elsevier has created a COVID-19 resource centre with free information in English and Mandarin on the novel coronavirus COVID-19. The COVID-19 resource centre is hosted on Elsevier Connect, the company's public news and information website.

Journal of Hazardous Materials 436 (2022) 129152

Contents lists available at ScienceDirect

Journal of Hazardous Materials

journal homepage: www.elsevier.com/locate/jhazmat

Research Paper

Evaluation of SARS-CoV-2 transmission in COVID-19 isolation wards: On-site sampling and numerical analysis

Wenjie Huang [a], Kailu Wang [b,c], Chi-Tim Hung [b,c], Kai-Ming Chow [d], Dominic Tsang [e], Raymond Wai-Man Lai [f], Richard Huan Xu [g], Eng-Kiong Yeoh [b,c], Kin-Fai Ho [b,*], Chun Chen [a,h,**]

[a] Department of Mechanical and Automation Engineering, The Chinese University of Hong Kong, Shatin, N.T. 999077, Hong Kong, China
[b] The Jockey Club School of Public Health and Primary Care, The Chinese University of Hong Kong, Shatin, N.T. 999077, Hong Kong, China
[c] Centre for Health Systems and Policy Research, JCSPHPC, The Chinese University of Hong Kong, Shatin, N.T. 999077, Hong Kong, China
[d] Department of Medicine and Therapeutics, Prince of Wales Hospital, Shatin, N.T. 999077, Hong Kong, China
[e] Public Health Laboratory Centre, Centre for Health Protection, Kowloon 999077, Hong Kong, China
[f] Department of Microbiology, Prince of Wales Hospital, Shatin, N.T. 999077, Hong Kong, China
[g] Department of Rehabilitation Science, Faculty of Health and Social Science, The Hong Kong Polytechnic University, Kowloon 999077, Hong Kong, China
[h] Shenzhen Research Institute, The Chinese University of Hong Kong, Shenzhen 518057, China

HIGHLIGHTS

- SARS-CoV-2 was detected in both air and surface samples in isolation wards.
- The dispersion and deposition of exhaled particles were analyzed by CFD simulation.
- Sampling and simulation supported the possibility of airborne transmission.
- Use of ceiling-mounted air cleaners is an effective intervention strategy in wards.
- Curtains separate adjacent patients but increase the risk of opposite patients.

GRAPHICAL ABSTRACT

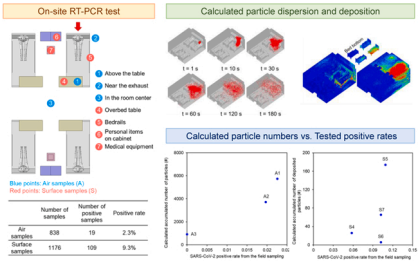

ARTICLE INFO

Editor: Danmeng Shuai

Keywords:
Aerosol transmission
Computational fluid dynamics (CFD)
Indoor environment
RT-PCR test
SARS-CoV-2

ABSTRACT

Although airborne transmission has been considered as a possible route for the spread of SARS-CoV-2, the role that aerosols play in SARS-CoV-2 transmission is still controversial. This study evaluated the airborne transmission of SARS-CoV-2 in COVID-19 isolation wards at Prince of Wales Hospital in Hong Kong by both on-site sampling and numerical analysis. A total of 838 air samples and 1176 surface samples were collected, and SARS-CoV-2 RNA was detected using the RT-PCR method. Testing revealed that 2.3% of the air samples and 9.3% of the surface samples were positive, indicating that the isolation wards were contaminated with the virus. The dispersion and deposition of exhaled particles in the wards were calculated by computational fluid dynamics (CFD) simulations. The calculated accumulated number of particles collected at the air sampling points was closely correlated with the SARS-CoV-2 positive rates from the field sampling, which confirmed the possibility of airborne transmission. Furthermore, three potential intervention strategies, i.e., the use of curtains, ceiling-mounted air cleaners, and periodic ventilation, were numerically investigated to explore effective control

* Corresponding author.
** Corresponding author at: Department of Mechanical and Automation Engineering, The Chinese University of Hong Kong, Shatin, N.T. 999077, Hong Kong, China.
E-mail addresses: kfho@cuhk.edu.hk (K.-F. Ho), chunchen@mae.cuhk.edu.hk (C. Chen).

https://doi.org/10.1016/j.jhazmat.2022.129152
Received 5 April 2022; Received in revised form 6 May 2022; Accepted 11 May 2022
Available online 14 May 2022

measures in isolation wards. According to the results, the use of ceiling-mounted air cleaners is effective in reducing the airborne transmission of SARS-CoV-2 in such wards.

1. Introduction

Coronavirus disease 2019 (COVID-19), a highly transmissible and pathogenic viral infection caused by severe acute respiratory syndrome coronavirus 2 (SARS-CoV-2), has spread globally, causing more than 5.6 million deaths as of February 2022 (World Health Organization). It is crucial to understand the transmission routes and characteristics of the virus for effective infection intervention. Close contact and respiratory droplets have been proven to be the main transmission modes of the SARS-CoV-2 virus (World Health Organization, 2020). In addition, airborne transmission via aerosols has been suggested as an important transmission pathway for SARS-CoV-2 (World Health Organization, 2020; Morawska and Milton, 2020).

Airborne transmission is defined as the spread of infectious aerosols (usually droplet nuclei) over long distances and times (World Health Organization, 2014). Aerosols are usually generated during medical treatment, and can also be produced by coughing, sneezing, and talking (Kutter et al., 2018; Stadnytskyi et al., 2020; Anfinrud et al., 2020). In outdoor environments, exhaled aerosols can be quickly diluted, so the probability of airborne transmission is very low, except for crowded public sites (Chirizzi et al., 2021; Belosi et al., 2021). However, in indoor environments, especially those with high occupancy and poor ventilation, the airborne transmission could be an issue (Dai and Zhao, 2020; Dinoi et al., 2021). Van Doremalen et al. Van Doremalen et al. (2020) found that SARS-CoV-2 could remain viable in aerosols for 3 h under the tested experimental conditions. Multiple studies (Liu et al., 2020; Chia et al., 2020; Lednicky et al., 2020; Guo et al., 2020; Zhou et al., 2021) have detected SARS-CoV-2 viral RNA in air samples. Liu et al. (2020) collected air samples in two Wuhan hospitals and found that aerosols with sizes in the sub-micrometre (0.25–1.0 μm) and super-micrometre (> 2.5 μm) ranges had the highest viral concentrations. Chia et al. (2020) detected SARS-CoV-2 PCR-positive airborne particles in isolation rooms with a high ventilation rate of 12 air changes per hour (ACH). Lednicky et al. (2020) demonstrated that the SARS-CoV-2 virus can be viable in aerosols by inoculating cells with the virus from air samples collected in hospitals. The recent review by Dinoi et al. (2021) found that people in hospitals and healthcare facilities are at higher risks of airborne SARS-CoV-2 transmission than in other indoor environments. These studies have indicated that airborne transmission of SARS-CoV-2 is possible. However, according to other studies, the airborne transmission mode for SARS-CoV-2 is still controversial (World Health Organization, 2020; Chagla et al., 2021; Asadi et al., 2020; Faridi et al., 2020). For instance, the role of droplet and fomite transmission cannot be ruled out in airborne transmission-related outbreaks and virus detections; the infection dose of inhaled viable virus is unknown; and the role of aerosols in transmission is also unknown. Therefore, it is still worthwhile to evaluate the airborne transmission of SARS-CoV-2 in order to add data and knowledge to this field.

In addition to on-site sampling, numerical simulations using computational fluid dynamics (CFD) are an effective method for investigating the aerodynamic characteristics of particle transport (Chen and Zhao, 2010; Chen et al., 2010; Zhang and Chen, 2007). During the 2003 SARS outbreak, this method was widely used to investigate the airborne transmission of the virus and optimize airflow distribution design (Li et al., 2005; Yu et al., 2004; Zhao et al., 2005; Kao and Yang, 2006; Gao and Niu, 2006; Jiang et al., 2009). Li et al. (2005) numerically studied the role of air distribution in SARS transmission during the largest nosocomial outbreak in Hong Kong. Yu et al. (2004) analysed the temporal and spatial distributions of infected cases in a large community outbreak of SARS in Hong Kong by CFD simulation. Zhao et al. (2005) numerically analysed the transport of exhaled droplets from normal respiration and coughing in indoor environments. In recent studies, this method has also been used to investigate the airborne spread of COVID-19 in crowded indoor environments (Shao et al., 2021; Abuhegazy et al., 2020; Li et al., 2021; Wang et al., 2021; Zhou and Ji, 2021; Ren et al., 2021). For instance, Shao et al. (2021) assessed the infection risk of airborne transmission of COVID-19 in three indoor spaces: an elevator, a classroom, and a supermarket. Abuhegazy et al. Abuhegazy et al. (2020) numerically investigated aerosol transport and surface deposition in a realistic classroom environment. Li et al. (2021) simulated the spread of fine exhaled droplets and assessed the possibility of airborne transmission in a COVID-19 outbreak inside a restaurant in

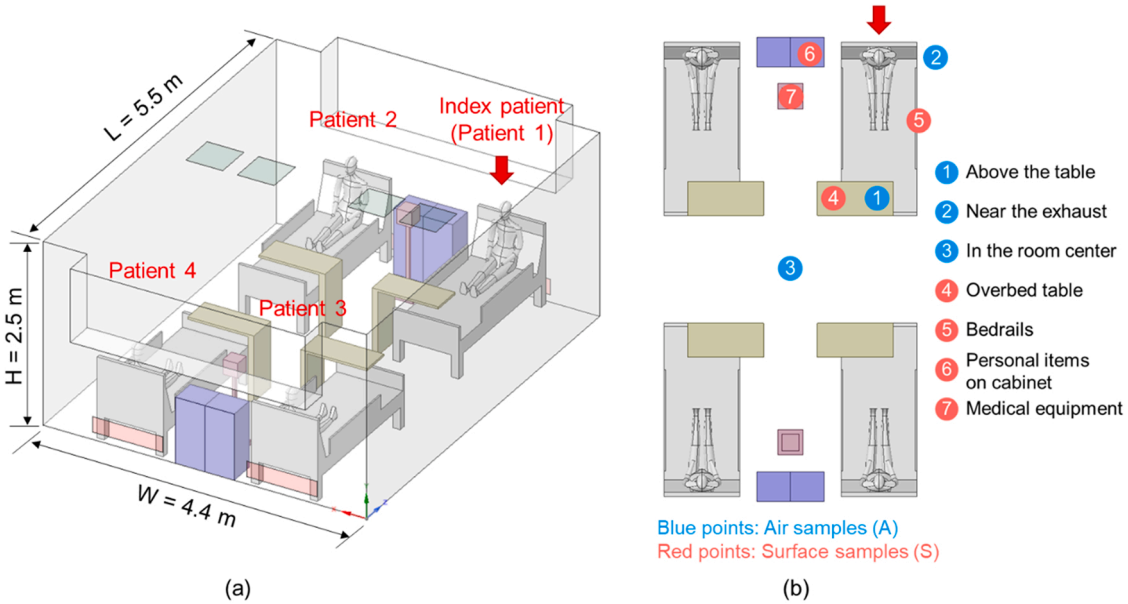

Fig. 1. (a) Configuration of the COVID-19 isolation ward and (b) locations of the sampling points.

Guangzhou, China. Wang et al. (2021) evaluated the transmission of SARS-CoV-2 via coughing, breathing, and talking during two real flights by CFD simulation. These studies have demonstrated that CFD simulations can be used to evaluate airborne transmission of SARS-CoV-2 in indoor environments.

This study aimed to evaluate the airborne transmission of SARS-CoV-2 in COVID-19 isolation wards at Prince of Wales Hospital in Hong Kong by both on-site sampling and numerical analysis. For the on-site sampling, the interference of droplets was ruled out by instructing the infected patients to cough while wearing a mask during sampling. A total of 838 air samples and 1176 surface samples were collected in the wards, and SARS-CoV-2 RNA was detected using the reverse transcription polymerase chain reaction (RT-PCR) method. The dispersion and deposition of exhaled particles in the wards were then calculated by CFD simulations. The calculated airborne particle concentrations and surface deposition accumulations were quantitatively compared with the SARS-CoV-2 positive rates from the field sampling to confirm the possibility of airborne transmission. Furthermore, three potential intervention strategies, i.e., the use of curtains, ceiling-mounted air cleaners, and periodic ventilation, were numerically investigated to explore effective control measures for reducing airborne transmission of SARS-CoV-2 in isolation wards.

2. On-site sampling of SARS-CoV-2 virus

2.1. Sampling methods

On-site sampling was conducted in the COVID-19 isolation wards at Prince of Wales Hospital in Hong Kong between August 2020 and March 2021. The sampling started in August 2020, the beginning of the 3rd wave of local COVID-19 epidemics. We targeted to collect at least 300 sets of air samples to obtain statistically meaningful results. However, due to the limited workforce in the fieldwork (the off-duty nurses with permission to enter the isolation wards), limited air sampling equipment, and decreasing trend of the epidemics, the sampling work was prolonged to March 2021 (the 4th wave of local epidemics). The sampling was conducted during this period whenever there were patients eligible and agreed to participate in the study and the fieldwork staff and sampling equipment were available. All samples were collected in 4-bed negative-pressure isolation wards with the same layout, as depicted in Fig. 1(a). Over 85% of the samples were taken when there were 3 or 4 COVID-19 confirmed patients in the isolation wards. The ventilation rate in the isolation wards was about 30 air changes per hour (ACH). The sampling locations are shown in Fig. 1(b). Three air samples and four surface samples were collected around a COVID-19 patient in each tested isolation ward, and were considered to be a set of samples. First, an air sample above the overbed table in front of the patient (A1 before cough) was collected. The patient was then instructed to cough three times while wearing a face mask to remove the coarse particles and exclude the interference of droplets. At the same time, two air samples were collected above the overbed table (A1) and near the ventilation exhaust (A2). Four surface samples were collected after the coughs, from the surfaces of the overbed table (S4), bedrails (S5), personal items (primarily the patient's mobile phone) on the bedside cabinet (S6), and medical equipment (S7). An additional air sample was collected in the center of the isolation ward (A3) once a week. Control group air samples were collected in an empty isolation ward. The air samples were collected using a Sartorius AirPort MD8 air sampler (Sartorius AG, Germany) with sterile gelatin filters (80 mm in diameter, Sartorius AG). Collection of each air sample lasted for 20 min with an airflow rate of 50 litre per minute. The surface samples were collected with premoistened swabs using an approach similar to that in previous studies (Dargahi et al., 2021; Harvey et al., 2020; Razzini et al., 2020). All the samples were analyzed by the RT-PCR method for detection of SARS-CoV-2 RNA (Hung et al., 2021). The sample recovery and RNA extraction followed the instructions by Santarpia et al. (2020). The limit of detection (LOD) of the approach in this study is 10 copies/ml in gelatin suspension.

Table 1
SARS-CoV-2 test results for the air and surface samples collected in the COVID-19 isolation wards.

	Sampling location	Number of samples	Number of positive samples	Positive rate
Air samples	Above overbed table (before cough) (A1)	311	8	2.6%
	Above overbed table (A1)	310	7	2.3%
	Near ventilation outlet (A2)	203	4	2.0%
	In the center of the ward (A3)	14	0	0.0%
Surface samples	Overbed table (S4)	294	17	5.8%
	Bedrails (S5)	294	32	10.9%
	Personal items on cabinet (S6)	294	30	10.2%
	Medical equipment (S7)	294	30	10.2%

2.2. Sampling results

A total of 311 sets of samples were collected in the isolation wards, including 838 air samples and 1176 surface samples, for which the test results are listed in Table 1. Among the control group air samples collected in the empty isolation ward, there was zero positive SARS-CoV-2 detection. There was little difference in the SARS-CoV-2 positive rate for the air samples collected on the overbed table before and after coughing. Thus, even without coughing, normal breaths from COVID-19 patients might also emit SARS-CoV-2 virus into the air. The air samples collected above the overbed tables had the highest SARS-CoV-2 positive rates (2.6% and 2.3% before and after coughing, respectively), followed by the air samples collected near the ventilation exhausts, with a positive rate of 2.0%. No SARS-CoV-2 positive air samples were collected in the center of the wards. Since all the patients were required to wear masks when coughing, the coarse particles that might carry more viral load tended to be filtered by the masks or deposit near the source. Therefore, the zero positive rate indicated that the concentrations in the center of the wards were too low to be detected by the sampling method. Meanwhile, according to test results for the surface samples, the bedrails were most likely to be polluted with SARS-CoV-2 virus, with the highest positive rate of 10.9%, followed by the personal items on the bedside cabinet and the medical equipment (10.2%) and the overbed table (5.8%). The SARS-CoV-2 positive rates for the surface samples tended to be higher than those for the air samples, which consisted with the findings in the review by Dinoi et al. (2021). The difference between the air and surface samples can be attributed to two reasons. First, the surface deposition of SARS-CoV-2 virus accumulated over time, which resulted in a greater amount of virus loading. In contrast, the airborne SARS-CoV-2 virus was continuously removed by the ventilation system and did not accumulate over time. Second, the exhaled particles with large sizes tended to deposit on the surfaces, which could carry a higher viral load.

3. Numerical simulation of SARS-CoV-2 transmission

To better understand SARS-CoV-2 transmission, this study conducted numerical simulations of exhaled particle dispersion and deposition in the COVID-19 isolation wards and compared the calculations with the sampling results.

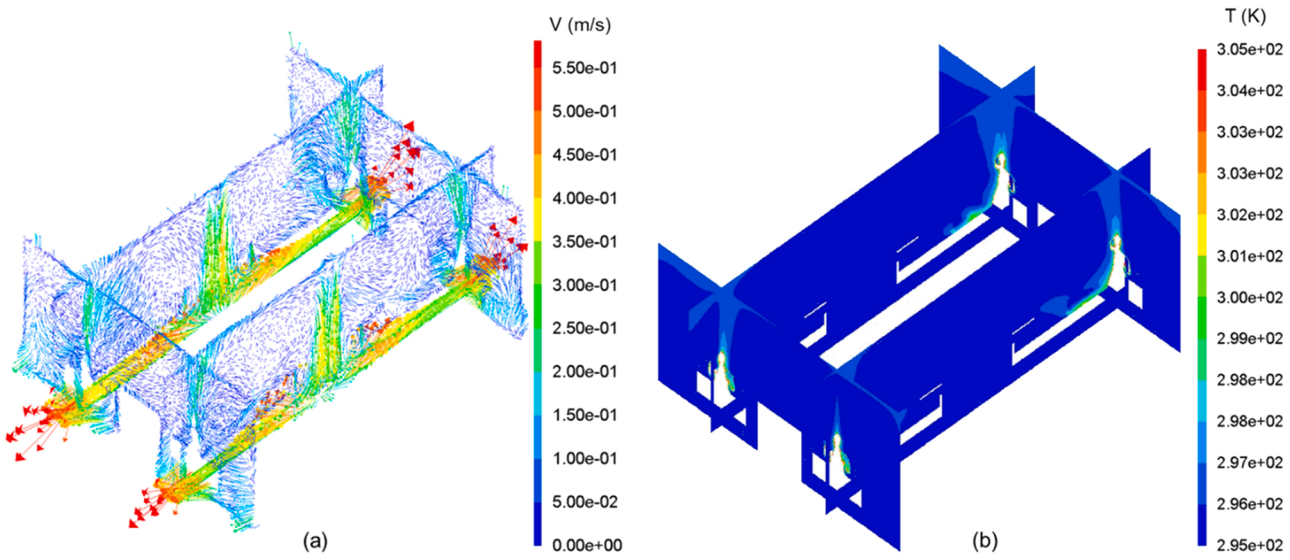

Fig. 2. Distributions of (a) airflow and (b) temperature at the four planes in the COVID-19 isolation ward.

3.1. Numerical models

3.1.1. Airflow and turbulence model

This study used the renormalization group (RNG) k-ε model to calculate the airflow and turbulence as recommended by Zhang et al. (2007), Wang and Chen (2009) and Chen (1995). The governing equations can be expressed in a general form as:

$$\frac{\partial(\rho\varnothing)}{\partial t}+\frac{\partial}{\partial x_i}\left[\rho u_i\varnothing-\Gamma_{\phi,eff}\frac{\partial\varnothing}{\partial x_i}\right]=S_\phi \tag{1}$$

where ∅ represents the independent variables: time-averaged velocity components ($\overline{u}_i$), turbulent kinetic energy (k), dissipation rate of turbulent kinetic energy (ε), and enthalpy (H). When ∅ is equal to unity, the equation represents the conservation of mass. Meanwhile, ρ is the air density, u_i is the Reynolds-averaged air velocity, $\Gamma_{\phi,eff}$ is the effective diffusion coefficient, x_i is the Cartesian direction, S_ϕ is the source term, and t is time.

3.1.2. Particle transport model

The Lagrangian model was used to calculate the particle dispersion and deposition. The trajectory of each individual particle was calculated according to the particle momentum equation:

$$\frac{d\vec{u}_p}{dt}=F_D\left(\vec{u}-\vec{u}_p\right)+\frac{\vec{g}(\rho_p-\rho)}{\rho_p}+\vec{F_a} \tag{2}$$

where $\vec{u}_p$ is the particle velocity vector, $\vec{u}$ is the air velocity vector, $F_D\left(\vec{u}-\vec{u}_p\right)$ is the drag force, $\vec{g}(\rho_p-\rho)/\rho_p$ represents the gravity and the buoyancy, $\vec{g}$ is the gravitational acceleration vector, ρ_p is the particle density, ρ is the air density, and $\vec{F_a}$ stands for additional forces per unit mass, including the Brownian force and Saffman lift force, of which the mathematical expressions can be found in the Fluent manual (Ansys inc, 2013). The inverse of relaxation time (F_D) can be calculated by:

$$F_D=\frac{18\mu}{\rho_p d_p^2 C_c} \tag{3}$$

where μ is the air viscosity, d_p is the particle diameter, and C_c is the Cunningham correction to Stokes' drag law, which can be calculated by:

$$C_c=1+\frac{\lambda}{d_p}\left(2.514+0.8\exp\left(-0.55\frac{d_p}{\lambda}\right)\right) \tag{4}$$

Here λ is the mean free path of air molecules. The particle trajectory was determined by both the time-averaged fluid velocity ($\overline{\vec{u}}$) and the instantaneous fluid velocity ($\overline{\vec{u}}'$). The $\overline{\vec{u}}$ was calculated by solving the Reynolds-averaged Navier-Stokes (RANS) equations. The discrete random walk (DRW) model was used to model $\overline{\vec{u}}'$:

$$\overline{\vec{u}}'=\zeta\sqrt{2k/3} \tag{5}$$

where ζ is a normally distributed random number. In this study, particle resuspension was not considered; thus, the trajectory calculation was terminated when the particle reached a surface, and the deposited particles were counted for each computing mesh on all the surfaces. This study first calculated the transient particle transport from a single injection pulse. The superimposition method (Chen et al., 2015; Chen et al., 2015; Gupta et al., 2011) was then used to convert the transient particle concentration from a single injection pulse to the particle concentration from continuous breathing or a cough. The commercial program ANSYS Fluent 15.0 (Ansys inc, 2013) was used to solve the governing equations. The airflow and particle transport models have been validated by experimental data in our previous studies (Chen et al., 2015, 2013).

3.2. Case setup

A geometric model of the 4-bed ward was built according to the field layout and dimensional measurements, as shown in Fig. 1(a). Only the main pieces of furniture were considered, including beds, overbed tables and bedside cabinets, in addition to medical equipment. The anteroom and bathroom were excluded from the calculations, since the doors were closed during sampling. Four air-supply inlets (500 mm × 500 mm) were located on the ceiling and are marked as green squares in Fig. 1(a); four exhausts (960 mm × 210 mm) were located on the wall behind each bed and are marked as pink rectangles. The supply air velocity and temperature were 0.5 m/s and 22 ℃, respectively. The turbulence intensity and turbulent viscosity ratio of the inlets were assumed to be 5% and 10, respectively. The temperature of the human body was set at 32 ℃. The walls were considered to be adiabatic. The enhanced wall treatment was used to resolve the airflow in the near-wall region. The solutions were considered to be converged when the residuals became

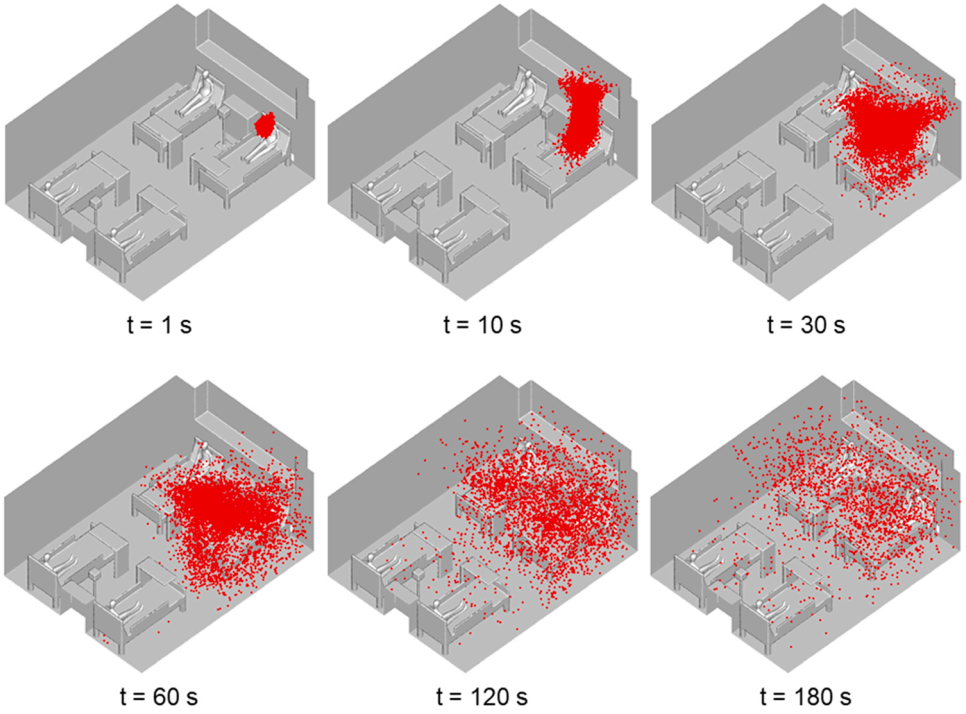

Fig. 3. Motion of the exhaled particles from a cough by the index patient (animation can be found in the Supplementary Materials).

less than 10^{-6} for energy and 10^{-4} for all other variables. According to the results of a grid-independence test, the grid number and time step size were set at 6.91 million (three grids were compared, i.e., 3.55 million, 6.91 million, and 10.84 million) and 0.1 s, respectively.

Since all the patients were required to wear masks when coughing, the momentum of the cough was neglected in the calculations (Tang et al., 2009; Chen et al., 2014). Furthermore, since coarse particles can be effectively removed by masks (Milton et al., 2013), the simulations only considered the dispersion of fine particles. Therefore, the particle diameter was set at 0.4 μm according to the mean size of exhaled particles through breathing (Gupta et al., 2011). Since both measurements and simulations confirmed that particles with a diameter less than 3 μm would disperse in a similar manner (Chen and Zhao, 2010; Yin et al., 2009), setting the particle size at 0.4 μm can yield the representative dispersion patterns. Particles were injected into the breathing zone with dimensions of 0.3 × 0.3 × 0.3 m^3 in front of the index patient's mouth as a single pulse, and the trajectories of the particles were tracked throughout the sampling period of 20 min. The superimposition method (Chen et al., 2015; Chen et al., 2015; Gupta et al., 2011) was then used to calculate the accumulated number of particles collected at the sampling points during the sampling period. The number of exhaled particles was set at 150 #/s for breathing and at 10^6 in 0.1 s for a cough (Gupta et al., 2011). Since the patients were instructed to wear surgical masks during the sampling, the particle removal efficiency of the masks was considered in the calculations and assumed to be 50% (Lai et al., 2012; Lindsley et al., 2021; Konda et al., 2020; Huo and Zhang, 2021). Since it is unclear how many SARS-CoV-2 virus were exhaled by a breath and a cough, respectively, it may not be meaningful to compare the calculated exhaled particle concentrations from different exhalation activities. Therefore, this study only compared the calculated accumulated particle numbers at the sampling points after the coughing. After the coughing, air samples were taken at A1, A2, and A3, with a sampling air volume of 1 m^3. Surface samples were collected on the upper surfaces of the overbed table (S4) and the bedside cabinet (S6), both sides of the two bedrails (S5), and the surfaces (excluding the bottom) of the medical equipment (S7), with a sampling area of 0.01 m^2.

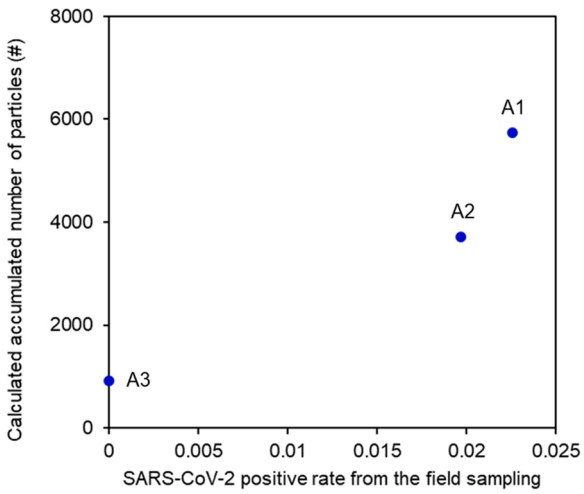

Fig. 4. Comparison of the calculated accumulated number of particles collected at the air sampling points during the 20-min sampling period with the SARS-CoV-2 positive rate from the field sampling.

3.3. Results

The airflow and temperature distributions are shown in Fig. 2. Clean air was supplied from the ceiling towards the floor, then moved along the floor to the side walls. Some air was exhausted through the exhausts behind the beds, while some rose to the ceiling due to the upward thermal plume generated by the patients, forming a circulation. Fig. 3 depicts the motion of the exhaled particles from a cough by the index patient, and the animation of this motion can be found in the Supplementary Materials. The exhaled particles first moved upward and dispersed with the airflow. When the particles approached the supply air inlets, they were blown down towards the floor by the jets. Some of the particles were removed through the exhausts with the airflow, while the remainder of the particles rose back into the recirculation zone. The

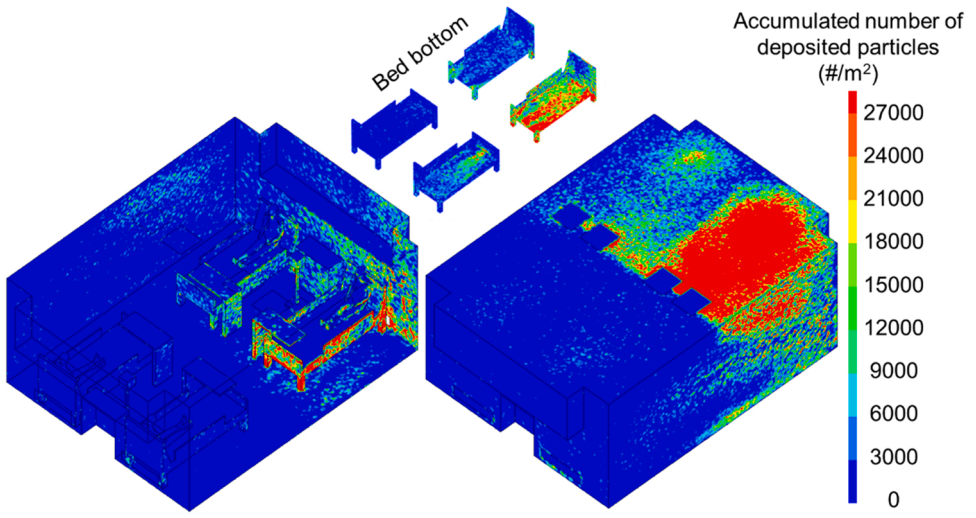

Fig. 5. Distribution of the number of deposited particles per unit area that accumulated during the 20-min sampling period.

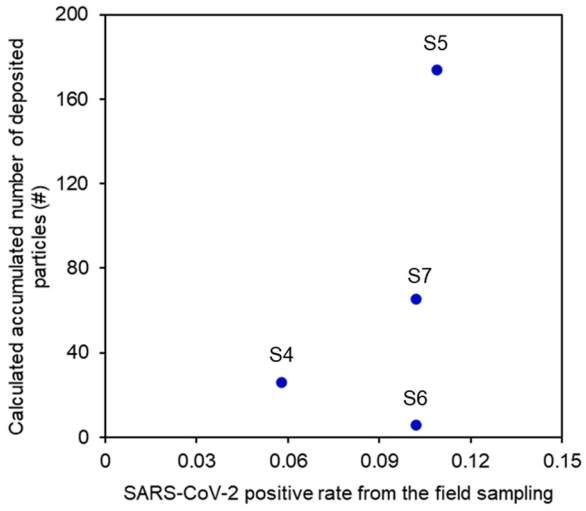

Fig. 6. Comparison of the calculated number of deposited particles that accumulated during the 20-min sampling period with the SARS-CoV-2 positive rates from the field sampling.

clean air jetting from the ceiling acted as an air curtain in the middle of the ward, dividing the ward into two zones. Most of the exhaled particles stayed on the side of the ward occupied by the index patient and patient 2. Fig. 4 depicts the correlation between the calculated accumulated number of particles collected at the air sampling points during the 20-min sampling period and the SARS-CoV-2 positive rate from the field sampling. The results show that A1 (the sample above the table) had the highest accumulated particle number, followed by A2 (the sample near the exhaust), while A3 (the sample in the center of the room) had the lowest accumulated particle number; these calculations were consistent with the SARS-CoV-2 positive rates from the field sampling.

Fig. 5 shows the distribution of the number of deposited particles per unit area that accumulated during the 20-min sampling period on different surfaces in the ward. Most of the exhaled particles deposited on the ceiling above the index patient due to the thermal plume generated by this patient. In addition, many particles deposited on the walls and furniture surfaces around the index patient, especially on the bed. Note that there were few particles deposited on the top surfaces of the bed and other furniture, but a large number of particles deposited on the side surfaces of the furniture and the bottom of the index patient's bed. This was because the exhaled particles first moved to the ceiling with the thermal plume, and then were quickly carried to the bottom of the ward by the supply air jets. Finally, the particles moved toward the exhausts with the airflow underneath the bed. Fig. 6 qualitatively compares the calculated number of deposited particles that accumulated during the 20-min sampling period with the SARS-CoV-2 positive rates from the

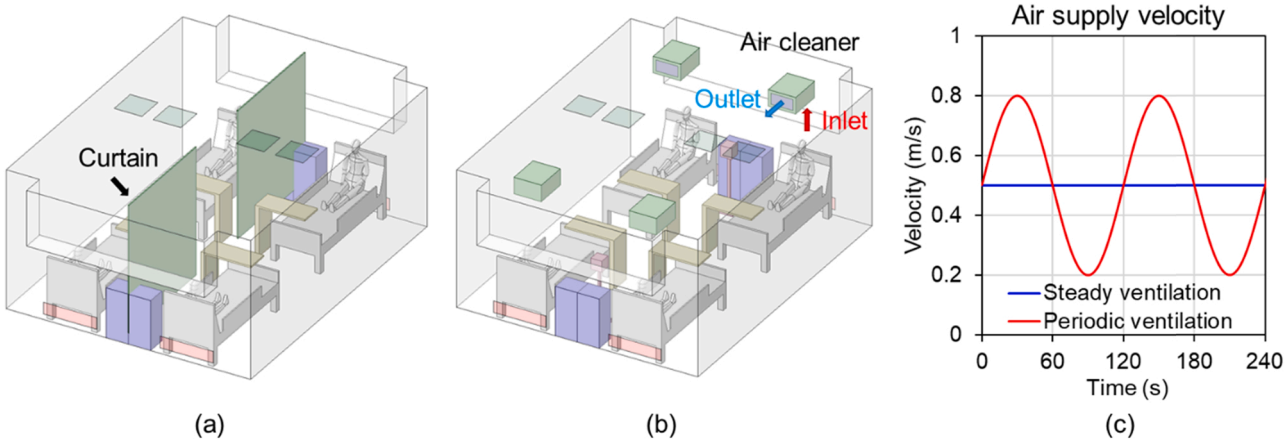

Fig. 7. Configurations for three potential intervention strategies: (a) use of curtains, (b) use of ceiling-mounted air cleaners, and (c) use of periodic ventilation.

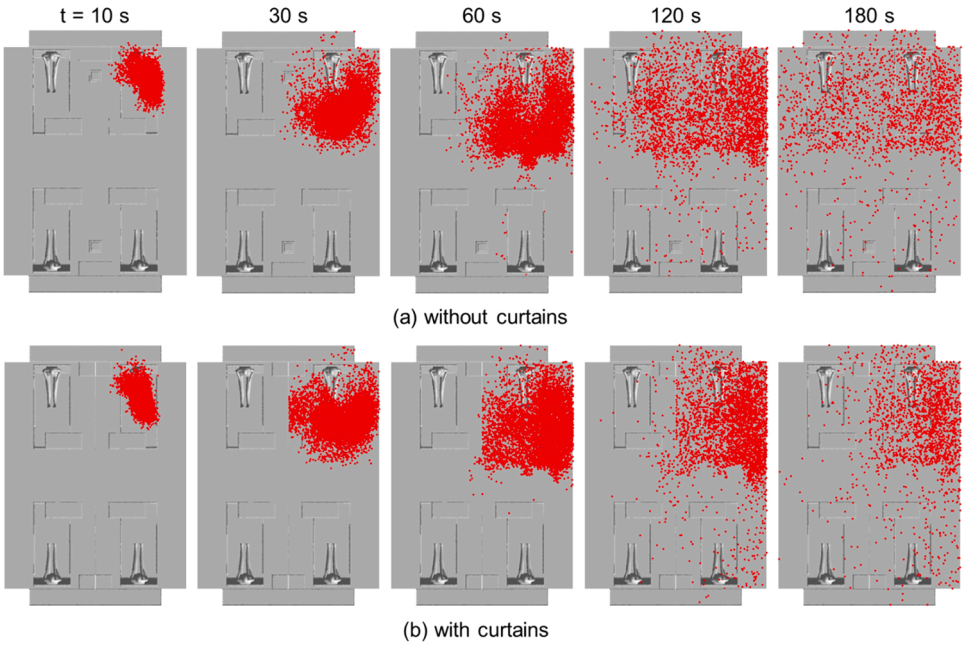

Fig. 8. Motion of the exhaled particles from a cough by the index patient: (a) without curtains and (b) with curtains (animation can be found in the Supplementary Materials).

field sampling. Surface S5 (bedrails) had the highest particle deposition amount, while the values for S7 (medical equipment) and S4 (table) were smaller, and that for S6 (the personal items on bedside cabinet) was the lowest. However, in the field measurements, S5, S6, and S7 all exhibited a high positive rate, while that of S4 was relatively low. In general, the correlation between the on-site sampling and numerical results was weak. This was probably because the patients and medical staff frequently touched the personal items and medical equipment with the virus on their hands, and this contact was not considered in the numerical simulations.

According to the results from on-site sampling and numerical simulation, the isolation wards were contaminated with SARS-CoV-2 aerosols exhaled by the index patient, even under a high ventilation rate of 30 ACH. The exhaled particles from the patient's cough dispersed quickly throughout the whole ward within five minutes, even with mask wearing. To better protect the other patients and heath care workers, it would be worthwhile to propose potential intervention strategies for controlling the dispersion of exhaled particles in isolation wards.

4. Evaluation of potential interventions

4.1. Case setup

This study further numerically evaluated three potential intervention strategies for controlling the dispersion of exhaled particles in the isolation ward, as shown in Fig. 7. The first strategy was to use curtains to control the exhaled particle dispersion. The supply air jets already provided effective air curtains at the plane $z = L/2$. Therefore, two curtains, each with dimensions of 2.3 m × 2.1 m (0.2 m above the floor), were hung at the plane $x = W/2$ to block particle dispersion between adjacent patients, as shown in Fig. 7(a). The second intervention strategy was to use air cleaners to remove the exhaled particles. According to the results in Section 3.2, the exhaled particles were carried to the ceiling by the upward thermal plume generated by the human body. Therefore, to remove the exhaled particles efficiently, four air cleaners (0.6 m × 0.5 m × 0.3 m) were installed on the ceiling, one above each patient's head, as shown in Fig. 7(b). For each air cleaner, the clean air

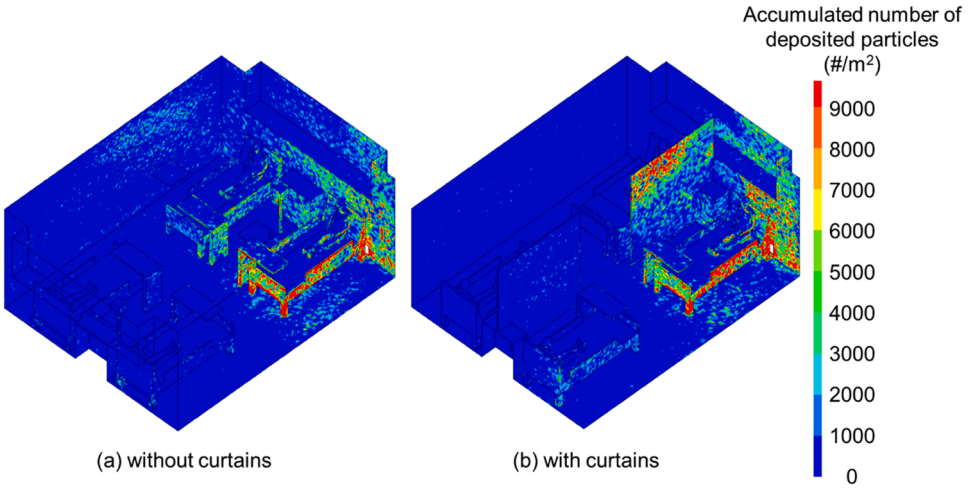

Fig. 9. Distributions of the number of deposited particles per unit area that accumulated in 10 min in the ward (a) without and (b) with curtains.

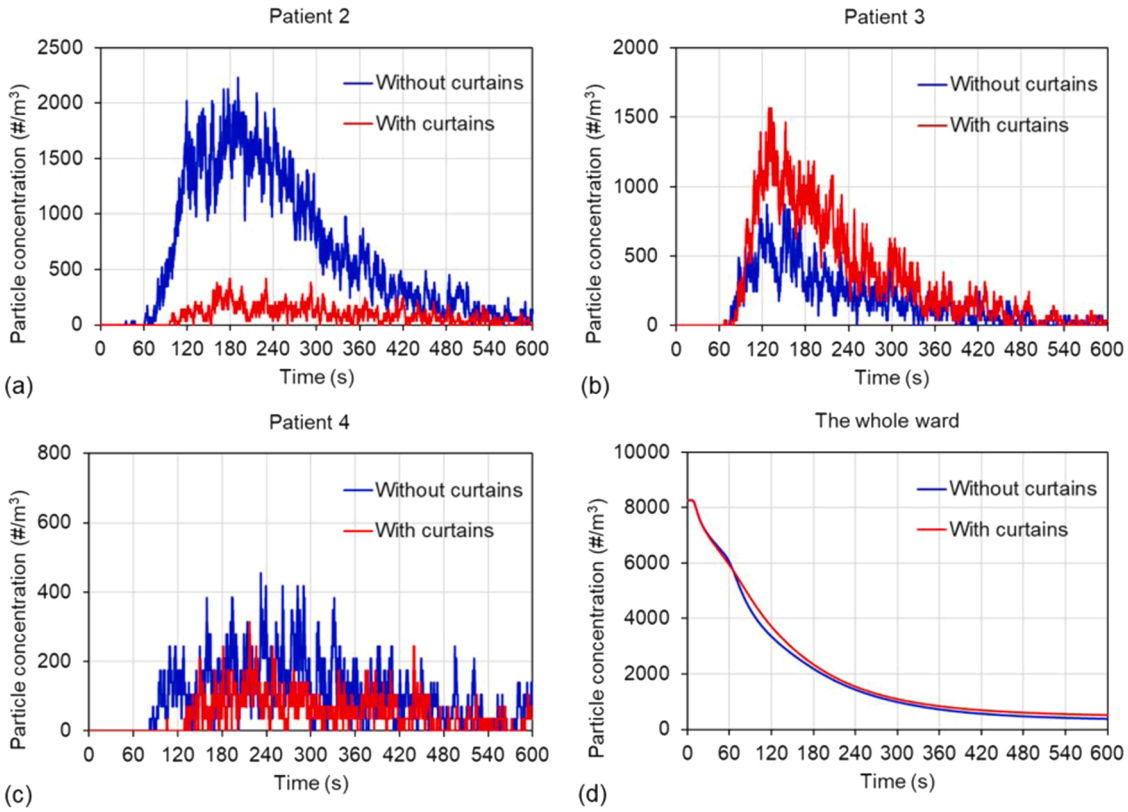

Fig. 10. Particle concentrations as a function of time (a)–(c) in the breathing zones of the other patients and (d) in the whole ward, with and without curtains.

delivery rate (CADR) was set at 100 m^3/h, and the particle removal efficiency was assumed to be 99.97% with the use of HEPA filters. The third intervention strategy was to use unsteady periodic ventilation, instead of steady ventilation, for higher ventilation efficiency as recommended by Huang et al. (2021), Van Hooff and Blocken (2020) and Kabanshi et al. (2016). A sinusoidal air supply with a period of 120 s was used for the periodic ventilation, as depicted in Fig. 7(c). For comparison of the infection risks, the particle concentrations from a cough by the index patient in each of the other patients' breathing zones (0.3 m × 0.3 m × 0.3 m in front of nose) and in the whole ward were recorded.

4.2. Curtains

Fig. 8 compares the motion of exhaled particles from a cough by the index patient with and without curtains. With the curtains, most of the particles stayed in the zone around the index patient, which greatly reduced the particle dispersion to patient 2. Consequently, as shown in

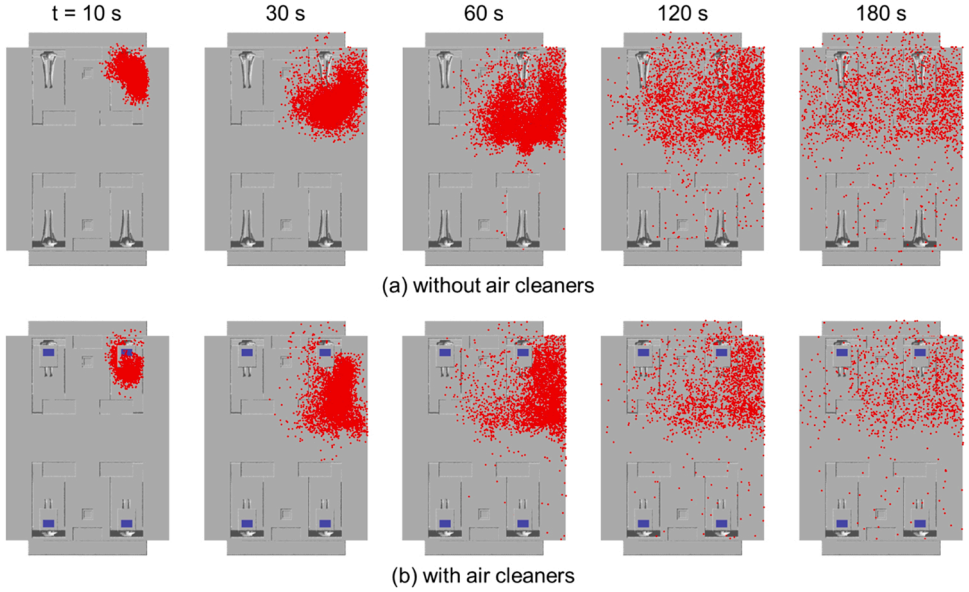

Fig. 11. Motion of the exhaled particles from a cough by the index patient: (a) without and (b) with ceiling-mounted air cleaners (animation can be found in the Supplementary Materials).

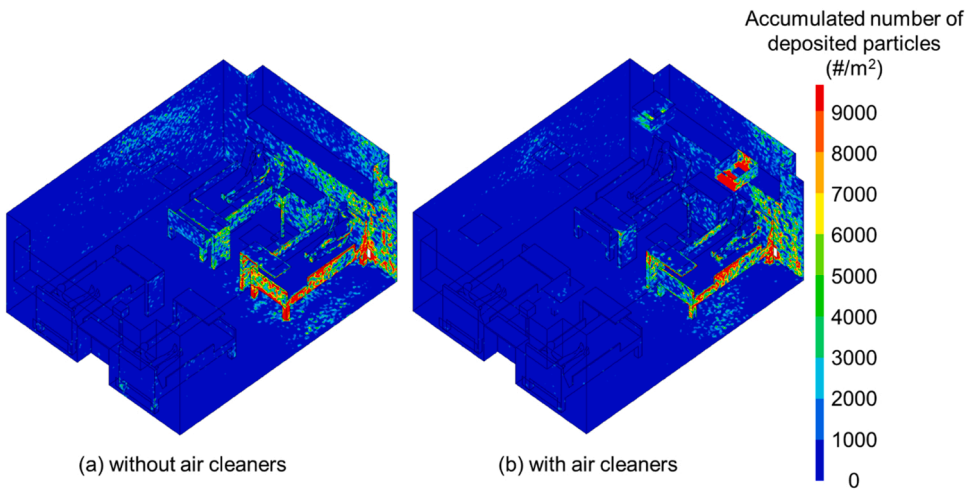

Fig. 12. Distributions of the number of deposited particles per unit area that accumulated in 10 min in the ward (a) without and (b) with ceiling-mounted air cleaners.

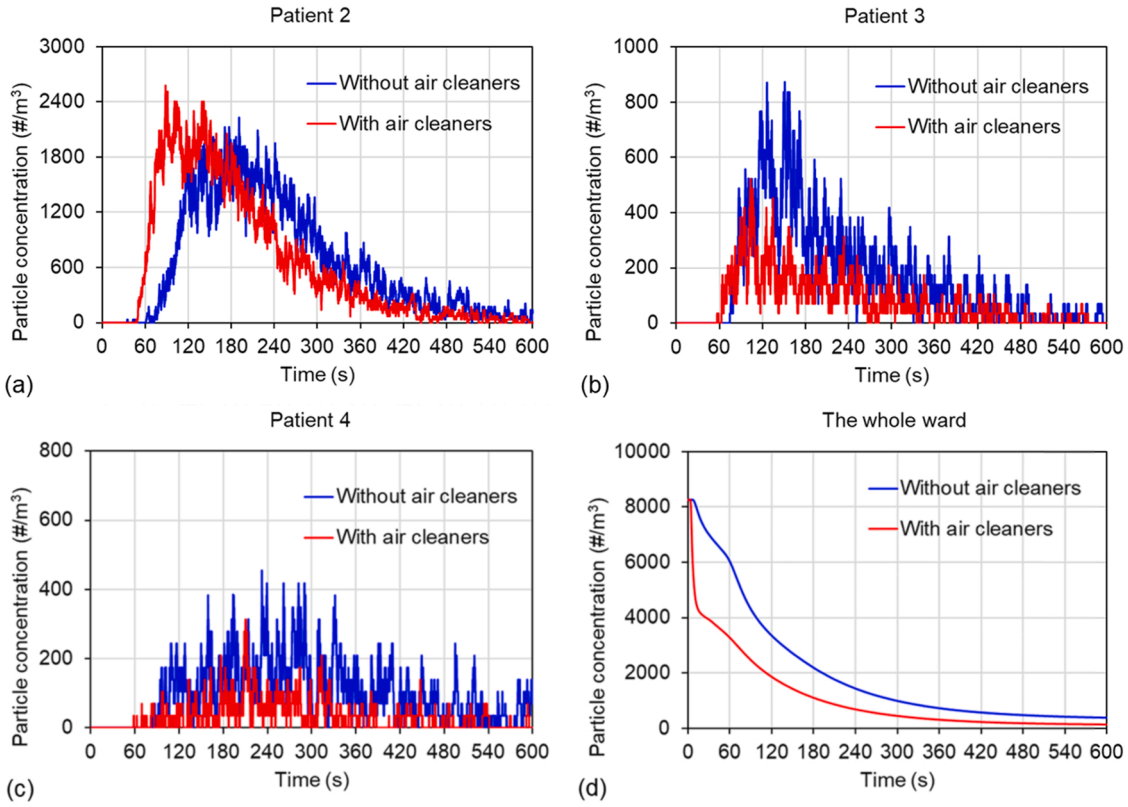

Fig. 13. Particle concentrations as a function of time (a)-(c) in the breathing zones of the other patients and (d) in the whole ward, with and without ceiling-mounted air cleaners.

Fig. 9, the number of deposited particles on the left side of the ward also decreased significantly. Fig. 10 illustrates the particle concentrations as a function of time in the breathing zones of the other patients and the whole ward with and without curtains. According to the results, using the curtains reduced the average particle concentration in the breathing zones of patients 2 and 4 by 87% and 52%, respectively. Meanwhile, as more particles were concentrated on the right side of the ward, the number of particles moving to the breathing zone of patient 3 slightly increased. Moreover, as shown in Fig. 10(d), after the curtains were added, the total particle number in the whole ward was similar to that without curtains because the curtains did not remove particles. In summary, using curtains in an isolation ward is beneficial for reducing potential cross-infection among the patients in the ward.

4.3. Air cleaners

Fig. 11 compares the motion of exhaled particles from a cough by the index patient with and without ceiling-mounted air cleaners. With the air cleaners, some exhaled particles were removed before they could spread throughout the ward. Furthermore, as shown in Fig. 12, the number of deposited particles that accumulated on the furniture surfaces and walls decreased because a considerable number of particles were

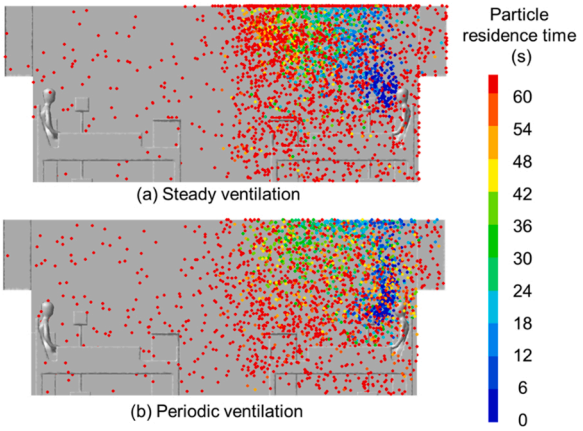

Fig. 14. Distribution and residence time of the exhaled particles from continuous breathing by the index patient at t = 10 min with (a) steady and (b) periodic ventilation.

removed by the air cleaners. Fig. 13 shows the particle concentrations in the breathing zones of the other patients and the whole ward, with and without air cleaners. Since the air cleaners increased the air velocity above each patient, the peaks of particle concentration in the patients' breathing zones occurred sooner, especially for patient 2 The average particle concentration in the breathing zones of patients 3 and 4 was reduced by 54% and 67%, respectively, while it did not change significantly for patient 2. Moreover, as shown in Fig. 13(d), the use of the ceiling-mounted air cleaners reduced the total particle number by 46% in the whole ward.

4.4. Periodic ventilation

This section compares the particle concentration and deposition under steady ventilation and periodic ventilation. Due to the varying supply air velocity of periodic ventilation, coughing at different points in time would lead to different results. Thus, continuous particle emission from breathing was adopted for the comparison of the two ventilation modes. Fig. 14 shows the distribution of exhaled particles from breathing by the index patient under steady and periodic ventilation at t = 10 min. Under steady ventilation, the exhaled particles were more concentrated in the upper zone in front of the index patient. Meanwhile, under periodic ventilation, the exhaled particles were distributed more widely and evenly. Moreover, the residence time of exhaled particles in the ward under periodic ventilation was shorter than that under steady ventilation. This was because the periodic ventilation enhanced the turbulence in the recirculation zone, which reduced the number of trapped particles. Fig. 15 shows the distributions of the number of deposited particles per unit area that accumulated in 10 min in the ward with steady and periodic ventilation. Under periodic ventilation, more particles deposited on the furniture surfaces, walls, and floor, as a result of the lower supply air velocity in the second half of the 10-min period. Fig. 16 shows the particle concentrations as a function of time in the breathing zones of the other patients and the whole ward under the two ventilation modes. The particle concentrations were steadier under steady ventilation, and fluctuated greatly under periodic ventilation. When the supply air velocity was low, more particles accumulated in the breathing zone of the index patient. When the supply air velocity increased, these accumulated particles dispersed, leading to peaks in the particle concentration in the breathing zones of the other patients, as depicted in Fig. 16(a)–(c). Moreover, Fig. 16(d) shows that the time-averaged particle concentration in the ward under periodic ventilation was lower than that under steady ventilation.

5. Discussion

In previous studies, respiratory droplets (> 5–10 μm) and close contact were considered to be the main transmission routes of the SARS-CoV-2 virus (World Health Organization, 2020). The role that aerosols (< 5 μm) might play in SARS-CoV-2 transmission is still controversial (World Health Organization, 2020; Chagla et al., 2021; Asadi et al., 2020; Faridi et al., 2020). According to the World Health Organization (WHO), aerosol transmission is possible, but the relationship between the exhaled aerosols and infection by SARS-CoV-2 is unknown (World Health Organization, 2020). Although some outbreaks in indoor environments have indicated the possibility of aerosol transmission, the WHO emphasized that the potential roles of droplet and fomite transmission could not be ruled out in these cases (World Health Organization, 2020). In the present study, on-site SARS-CoV-2 sampling and numerical analysis were conducted to investigate the airborne transmission of exhaled particles in COVID-19 isolation wards. During the on-site sampling, each patient was instructed to wear a mask when coughing to eliminate the effects of respiratory droplets. SARS-CoV-2 RNA was detected in 19 out of 838 air samples, indicating that the aerosol particles exhaled by the infected patients carried the virus. Moreover, the trajectories of exhaled particles (0.4 μm) from the index patient were numerically calculated under the same conditions as the on-site sampling. The calculated particle concentration was positively associated with the SARS-CoV-2 positive rate, which supported the possibility of airborne transmission of SARS-CoV-2. According to the

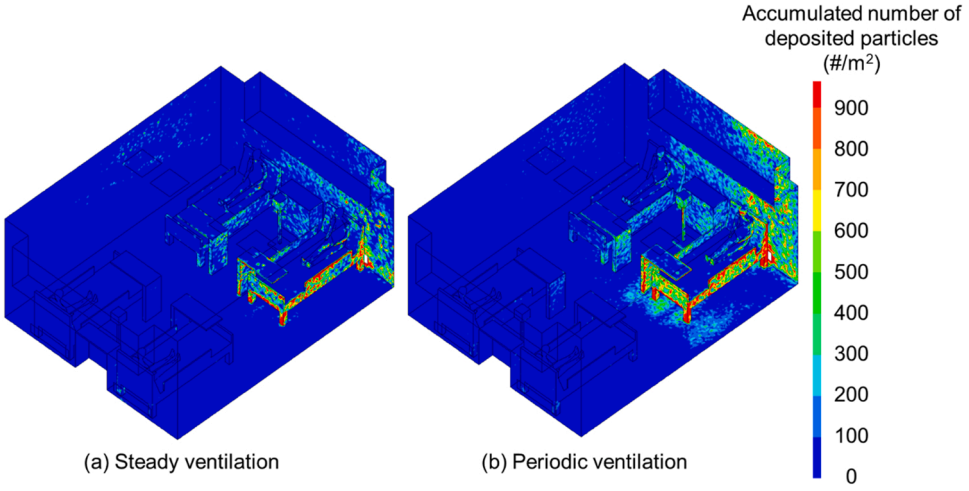

Fig. 15. Distributions of the number of deposited particles per unit area that accumulated in 10 min in the ward with (a) steady and (b) periodic ventilation.

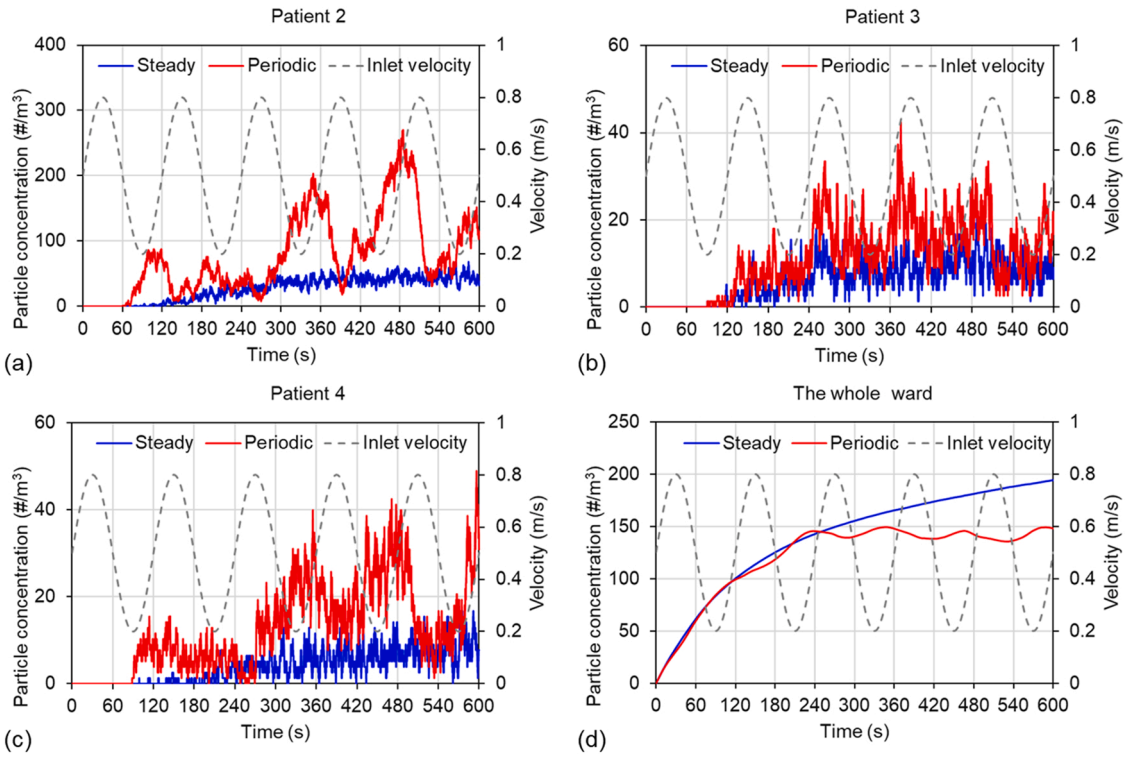

Fig. 16. Particle concentrations as a function of time (a)-(c) in the breathing zones of the other patients and (d) in the whole ward, under steady and periodic ventilation.

Table 2
Ratio of average particle concentration with each of the three intervention strategies to the concentration in the original case ($C/C_{original}$) in the breathing zones of the other patients and in the whole ward.

Zone	Curtain	Air cleaner	Periodic ventilation
Patient 2	13%	100%	285%
Patient 3	198%	46%	178%
Patient 4	48%	33%	319%
Patients 2 & 3 & 4	51%	83%	270%
Whole ward	107%	54%	87%

calculated results for airborne particle transport, most of the particles were concentrated in the upper part of the room above the index patient due to the thermal plume. Thus, airborne transmission in a hospital ward could be controlled effectively through the use of ceiling-mounted air cleaners to remove airborne particles from the upper part of the ward.

Meanwhile, SARS-CoV-2 was detected in 109 out of 1176 surface samples. Bedrails were the surface that was most likely to be polluted in both the tests (positive rate of 10.9%) and calculations, and this finding is consistent with test results from other studies (Chia et al., 2020; Razzini et al., 2020; Cheng et al., 2020). The personal items on the bedside cabinet (primarily the patient's mobile phone) and medical equipment also had a relatively high positive rate of 10.2%, but with lower accumulation of deposited particles; this positive rate may be related more closely to other transmission routes, such as contact transmission. The numerical results indicated that large numbers of particles deposited on the walls and furniture surfaces around the index patient, especially on the ceiling and bed. According to the calculated particle deposition distribution, some surfaces that may typically be overlooked, such as the side surfaces of furniture and the bottoms of beds, had even stronger particle deposition than the top surfaces. These results provide helpful guidance for more effective surface disinfection.

The particle concentrations in the breathing zones of the other patients and the whole room were numerically analysed to determine the effectiveness of the three intervention strategies in airborne infection control. For each of the three strategies, Table 2 lists the ratio of the average particle concentration with the control measure to the concentration in the original case ($C/C_{original}$). The use of curtains greatly reduced the airborne transmission of particles between adjacent patients. For patient 2 (next to the index patient), the mean particle concentration in the breathing zone was reduced by 87%, from 1270 #/m^3 to 166 #/m^3. However, the use of curtains also increased the infection risk of the opposite patient. The mean particle concentration in the breathing zone of patient 3 almost doubled. Therefore, the use of curtains is more suitable for two-bed wards. The use of air cleaners installed on the ceiling above each patient's head effectively reduced the total particle number in the ward by 46%, since nearly half of the particles exhaled by the index patient were carried by the upward thermal plume and directly removed by the air cleaners. The particle concentrations in the breathing zones of all the patients and in the whole ward decreased to some extent. In general, properly locating the air cleaners is important for effectively reducing the infectious risks (Chen et al., 2010; Dai and Zhao, 2022). It would be more effective to place the air cleaners near the index patients, because the exhaled particles could be directly removed without dispersing in the room. However, in some environments, the ideal location for air cleaners may not be available due to space or layout limitations. In this case, the relative position between the air cleaner and the patients should be carefully designed, as an improper air cleaner location may even result in increased infection risks (Chen et al., 2010). Moreover, according to Dai and Zhao (2022), it would be optimal to place the air cleaner in the center of the room if the airflow rate of air cleaner is large enough. Under periodic ventilation, as the varying airflow enhanced the particle dispersion, the average particle concentration increased in all the patients' breathing zones, while the total particle number in the ward decreased by 13%. In general, the use of curtains can effectively prevent mutual infection between patients in the same ward. Ceiling-mounted air cleaners can promptly remove exhaled particles and reduce the particle concentrations in patients' breathing zones and the whole ward, which is beneficial for protecting both the

patients and medical staff. Although periodic ventilation can reduce the trapping of particles in the recirculation zone, which may be helpful in protecting medical staff, it might increase the infection risk for the patients.

There are some limitations in this study. First, detection of SARS-CoV-2 RNA by the RT-PCR method does not indicate the existence of viable virus that could be transmissible and infectious (Santarpia et al., 2020; Bullard et al., 2020). Second, the relationship between COVID-19 infection risk and the concentration of exhaled airborne particles is unknown. Therefore, the airborne transmission of viable SARS-CoV-2 virus and the infectious dose of viable virus merit further study.

6. Conclusions

This study investigated the airborne transmission of SARS-CoV-2 in COVID-19 isolation wards at Prince of Wales Hospital by both on-site sampling using the RT-PCR method and numerical analysis using CFD simulations. The dispersion and deposition of exhaled particles were calculated for better understanding of airborne transmission. Three intervention strategies, including the use of curtains, ceiling-mounted air cleaners, and periodic ventilation, for airborne transmission control were then numerically investigated. The following conclusions can be drawn within the scope of this study:

1. In the on-site sampling, 2.3% of air samples and 9.3% of surface samples were tested as positive for SARS-CoV-2, indicating that the COVID-19 isolation wards were contaminated with the virus.
2. The calculated accumulated number of particles collected at the air sampling points in the sampling period was closely correlated with the SARS-CoV-2 positive rate from the field sampling.
3. The calculation results indicated that most of the exhaled particles were concentrated in the upper part of the ward, and most of the particle deposition occurred on the walls and furniture surfaces around the index patient.
4. The use of ceiling-mounted air cleaners is an effective intervention strategy for reducing the airborne transmission of SARS-CoV-2 in isolation wards. Moreover, the use of curtains can effectively reduce the cross-infection between the adjacent patients, but would increase the risk of the opposite patient.

Statement of environmental implication

SARS-CoV-2 is a strain of coronavirus responsible for the ongoing COVID-19 pandemic, which has caused more than 5.6 million deaths as of February 2022. Thus, SARS-CoV-2 virus and virus loaded airborne particles can be considered “hazardous material”. In this study, on-site SARS-CoV-2 sampling and numerical analysis were conducted to investigate the airborne transmission of exhaled particles in COVID-19 isolation wards. The results supported the possibility of airborne transmission of SARS-CoV-2 and provided helpful guidance for more effective infection intervention. Furthermore, three potential intervention strategies were numerically investigated to explore effective control measures for reducing airborne transmission of SARS-CoV-2 in wards.

CRediT authorship contribution statement

Wenjie Huang: Methodology, Investigation, Writing – original draft. **Kailu Wang:** Methodology, Investigation. **Chi-Tim Hung:** Methodology, Investigation. **Kai-Ming Chow:** Methodology, Investigation. **Dominic Tsang:** Methodology, Investigation. **Raymond Wai-Man Lai:** Methodology, Investigation. **Richard Huan Xu:** Methodology, Investigation. **Eng-Kiong Yeoh:** Methodology, Investigation. **Kin-Fai Ho:** Conceptualization, Methodology, Supervision, Writing – review & editing. **Chun Chen:** Conceptualization, Methodology, Supervision, Writing – review & editing.

Declaration of Competing Interest

The authors declare that they have no known competing financial interests or personal relationships that could have appeared to influence the work reported in this paper.

Acknowledgments

This work was partially supported by the General Research Fund of Research Grants Council of Hong Kong SAR, China (Grant No. 14204520), the Health and Medical Research Fund of Food and Health Bureau of Hong Kong SAR, China (Grant No. COVID190101), and CUHK Direct Grant (2020.021).

Appendix A. Supporting information

Supplementary data associated with this article can be found in the online version at doi:10.1016/j.jhazmat.2022.129152.

References

Abuhegazy, M., Talaat, K., Anderoglu, O., Poroseva, S.V., 2020. Numerical investigation of aerosol transport in a classroom with relevance to COVID-19. Phys. Fluids 32 (10), 103311.
Anfinrud, P., Stadnytskyi, V., Bax, C.E., Bax, A., 2020. Visualizing speech-generated oral fluid droplets with laser light scattering. New Engl. J. Med. 382 (21), 2061–2063.
Ansys Inc, 2013. ANSYS Fluent 15.0 Documentation.
Asadi, S., Bouvier, N., Wexler, A.S., Ristenpart, W.D., 2020. The coronavirus pandemic and aerosols: Does COVID-19 transmit via expiratory particles? Aerosol Sci. Technol. 54 (6), 635–638.
Belosi, F., Conte, M., Gianelle, V., Santachiara, G., Contini, D., 2021. On the concentration of SARS-CoV-2 in outdoor air and the interaction with pre-existing atmospheric particles. Environ. Res. 193, 110603.
Bullard, J., Dust, K., Funk, D., Strong, J.E., Alexander, D., Garnett, L., Poliquin, G., 2020. Predicting infectious severe acute respiratory syndrome coronavirus 2 from diagnostic samples. Clin. Infect. Dis. 71 (10), 2663–2666.
Chagla, Z., Hota, S., Khan, S., Mertz, D., International Hospital and Community Epidemiology Group, 2021. Re: it is time to address airborne transmission of COVID-19. Clin. Infect. Dis. 73 (11), e3981–e3982.
Chen, C., Zhao, B., 2010. Some questions on dispersion of human exhaled droplets in ventilation room: answers from numerical investigation. Indoor Air 20 (2), 95–111.
Chen, C., Zhao, B., Cui, W., Dong, L., An, N., Ouyang, X., 2010. The effectiveness of an air cleaner in controlling droplet/aerosol particle dispersion emitted from a patient's mouth in the indoor environment of dental clinics. J. R. Soc. Interface 7 (48), 1105–1118.
Chen, C., Liu, W., Li, F., Lin, C.-H., Liu, J., Pei, J., Chen, Q., 2013. A hybrid model for investigating transient particle transport in enclosed environments. Build. Environ. 62, 45–54.
Chen, C., Lin, C.H., Jiang, Z., Chen, Q., 2014. Simplified models for exhaled airflow from a cough with the mouth covered. Indoor Air 24 (6), 580–591.
Chen, C., Liu, W., Lin, C.H., Chen, Q., 2015. Comparing the Markov chain model with the Eulerian and Lagrangian models for indoor transient particle transport simulations. Aerosol Sci. Technol. 49 (10), 857–871.
Chen, C., Liu, W., Lin, C.H., Chen, Q., 2015. Accelerating the Lagrangian method for modeling transient particle transport in indoor environments. Aerosol Sci. Technol. 49 (5), 351–361.
Chen, Q., 1995. Comparison of different k-ε models for indoor air flow computations. Numer. Heat Transf. Part B Fundam. 28 (3), 353–369.
Cheng, V.C.C., Wong, S.C., Chan, V.W.M., So, S.Y.C., Chen, J.H.K., Yip, C.C.Y., Yuen, K. Y., 2020. Air and environmental sampling for SARS-CoV-2 around hospitalized patients with coronavirus disease 2019 (COVID-19). Infect. Control Hosp. Epidemiol. 41 (11), 1258–1265.
Chia, P.Y., Coleman, K.K., Tan, Y.K., Ong, S.W.X., Gum, M., Lau, S.K., Marimuthu, K., 2020. Detection of air and surface contamination by SARS-CoV-2 in hospital rooms of infected patients. Nat. Commun. 11 (1), 1–7.
Chirizzi, D., Conte, M., Feltracco, M., Dinoi, A., Gregoris, E., Barbaro, E., Contini, D., 2021. SARS-CoV-2 concentrations and virus-laden aerosol size distributions in outdoor air in north and south of Italy. Environ. Int. 146, 106255.
Dai, H., Zhao, B., 2020. Association of the infection probability of COVID-19 with ventilation rates in confined spaces. Build. Simul. 13 (6), 1321–1327.
Dai, H., Zhao, B., 2022. Reducing airborne infection risk of COVID-19 by locating air cleaners at proper positions indoor: Analysis with a simple model. Build. Environ. 213, 108864.
Dargahi, A., Jeddi, F., Vosoughi, M., Karami, C., Hadisi, A., Mokhtari, S.A., Sadeghi, H., 2021. Investigation of SARS CoV-2 virus in environmental surface. Environ. Res. 195, 110765.
Dinoi, A., Feltracco, M., Chirizzi, D., Trabucco, S., Conte, M., Gregoris, E., Contini, D., 2021. A review on measurements of SARS-CoV-2 genetic material in air in outdoor and indoor environments: Implication for airborne transmission. Sci. Total Environ. 809, 151137.

Faridi, S., Niazi, S., Sadeghi, K., Naddafi, K., Yavarian, J., Shamsipour, M., MokhtariAzad, T., 2020. A field indoor air measurement of SARS-CoV-2 in the patient rooms of the largest hospital in Iran. Sci. Total Environ. 725, 138401.
Gao, N., Niu, J., 2006. Transient CFD simulation of the respiration process and inter-person exposure assessment. Build. Environ. 41 (9), 1214–1222.
Guo, Z.D., Wang, Z.Y., Zhang, S.F., Li, X., Li, L., Li, C., Chen, W., 2020. Aerosol and surface distribution of severe acute respiratory syndrome coronavirus 2 in hospital wards, Wuhan, China, 2020. Emerg. Infect. Dis. 26 (7), 1586.
Gupta, J.K., Lin, C.H., Chen, Q., 2011. Transport of expiratory droplets in an aircraft cabin. Indoor Air 21 (1), 3–11.
Gupta, J.K., Lin, C.H., Chen, Q., 2011. Inhalation of expiratory droplets in aircraft cabins. Indoor Air 21 (4), 341–350.
Harvey, A.P., Fuhrmeister, E.R., Cantrell, M.E., Pitol, A.K., Swarthout, J.M., Powers, J.E., Pickering, A.J., 2020. Longitudinal monitoring of SARS-CoV-2 RNA on high-touch surfaces in a community setting. Environ. Sci. Technol. Lett. 8 (2), 168–175.
Huang, W., An, Y., Pan, Y., Li, J., Chen, C., 2021. Predicting transient particle transport in periodic ventilation using Markov chain model with pre-stored transition probabilities. Build. Environ., 108730
Hung, C.T., Yeoh, E.K., Ho, K.F., Tsang, D., Lai, W.M. R., Chow, K.M., Xu, R.H., & Wang, K. (2021). How high is the risk of environmental contamination and airborne infection of the SARS-CoV-2 virus? Health Research Symposium 2021, Hong Kong, 79–80 (No. COVID-15–135).
Huo, S., Zhang, T.T., 2021. Ventilation of ordinary face masks. Build. Environ. 205, 108261.
Jiang, Y., Zhao, B., Li, X., Yang, X., Zhang, Z., Zhang, Y., 2009. Investigating a safe ventilation rate for the prevention of indoor SARS transmission: an attempt based on a simulation approach. Build. Simul. 2 (4), 281–289.
Kabanshi, A., Wigö, H., Sandberg, M., 2016. Experimental evaluation of an intermittent air supply system–Part 1: thermal comfort and ventilation efficiency measurements. Build. Environ. 95, 240–250.
Kao, P.H., Yang, R.J., 2006. Virus diffusion in isolation rooms. J. Hosp. Infect. 62 (3), 338–345.
Konda, A., Prakash, A., Moss, G.A., Schmoldt, M., Grant, G.D., Guha, S., 2020. Aerosol filtration efficiency of common fabrics used in respiratory cloth masks. ACS Nano 14 (5), 6339–6347.
Kutter, J.S., Spronken, M.I., Fraaij, P.L., Fouchier, R.A., Herfst, S., 2018. Transmission routes of respiratory viruses among humans. Curr. Opin. Virol. 28, 142–151.
Lai, A.C.K., Poon, C.K.M., Cheung, A.C.T., 2012. Effectiveness of facemasks to reduce exposure hazards for airborne infections among general populations. J. R. Soc. Interface 9 (70), 938–948.
Lednicky, J.A., Lauzardo, M., Fan, Z.H., Jutla, A., Tilly, T.B., Gangwar, M., Wu, C.Y., 2020. Viable SARS-CoV-2 in the air of a hospital room with COVID-19 patients. Int. J. Infect. Dis. 100, 476–482.
Li, Y., Huang, X., Yu, I.T., Wong, T.W., Qian, H., 2005. Role of air distribution in SARS transmission during the largest nosocomial outbreak in Hong Kong. Indoor Air 15 (2), 83–95.
Li, Y., Qian, H., Hang, J., Chen, X., Cheng, P., Ling, H., Kang, M., 2021. Probable airborne transmission of SARS-CoV-2 in a poorly ventilated restaurant. Build. Environ. 196, 107788.
Lindsley, W.G., Blachere, F.M., Law, B.F., Beezhold, D.H., Noti, J.D., 2021. Efficacy of face masks, neck gaiters and face shields for reducing the expulsion of simulated cough-generated aerosols. Aerosol Sci. Technol. 55 (4), 449–457.
Liu, Y., Ning, Z., Chen, Y., Guo, M., Liu, Y., Gali, N.K., Lan, K., 2020. Aerodynamic analysis of SARS-CoV-2 in two Wuhan hospitals. Nature 582 (7813), 557–560.
Milton, D.K., Fabian, M.P., Cowling, B.J., Grantham, M.L., McDevitt, J.J., 2013. Influenza virus aerosols in human exhaled breath: particle size, culturability, and effect of surgical masks. PLoS Pathog. 9 (3), e1003205.
Morawska, L., Milton, D.K., 2020. It is time to address airborne transmission of coronavirus disease 2019 (COVID-19). Clin. Infect. Dis. 71 (9), 2311–2313.
Razzini, K., Castrica, M., Menchetti, L., Maggi, L., Negroni, L., Orfeo, N.V., Balzaretti, C. M., 2020. SARS-CoV-2 RNA detection in the air and on surfaces in the COVID-19 ward of a hospital in Milan, Italy. Sci. Total Environ. 742, 140540.
Ren, J., Wang, Y., Liu, Q., Liu, Y., 2021. Numerical study of three ventilation strategies in a prefabricated COVID-19 inpatient ward. Build. Environ. 188, 107467.
Santarpia, J.L., Rivera, D.N., Herrera, V.L., Morwitzer, M.J., Creager, H.M., Santarpia, G. W., Lowe, J.J., 2020. Aerosol and surface contamination of SARS-CoV-2 observed in quarantine and isolation care. Sci. Rep. 10 (1), 1–8.
Shao, S., Zhou, D., He, R., Li, J., Zou, S., Mallery, K., Hong, J., 2021. Risk assessment of airborne transmission of COVID-19 by asymptomatic individuals under different practical settings. J. Aerosol Sci. 151, 105661.
Stadnytskyi, V., Bax, C.E., Bax, A., Anfinrud, P., 2020. The airborne lifetime of small speech droplets and their potential importance in SARS-CoV-2 transmission. Proc. Natl. Acad. Sci. USA 117 (22), 11875–11877.
Tang, J.W., Liebner, T.J., Craven, B.A., Settles, G.S., 2009. A schlieren optical study of the human cough with and without wearing masks for aerosol infection control. J. R. Soc. Interface 6 (suppl_6), S727–S736.
Van Doremalen, N., Bushmaker, T., Morris, D.H., Holbrook, M.G., Gamble, A., Williamson, B.N., Munster, V.J., 2020. Aerosol and surface stability of SARS-CoV-2 as compared with SARS-CoV-1. New Engl. J. Med. 382 (16), 1564–1567.
Van Hooff, T., Blocken, B., 2020. Mixing ventilation driven by two oppositely located supply jets with a time-periodic supply velocity: a numerical analysis using computational fluid dynamics. Indoor Built Environ. 29 (4), 603–620.
Wang, M., Chen, Q., 2009. Assessment of various turbulence models for transitional flows in an enclosed environment (RP-1271). Hvacr Res. 15 (6), 1099–1119.
Wang, W., Wang, F., Lai, D., Chen, Q., 2021. Evaluation of SARS-COV-2 transmission and infection in airliner cabins. Indoor air 32 (1), e12979.
World Health Organization, 2020. Transmission of SARS-CoV-2: implications for infection prevention precautions: scientific brief, 09 July 2020. ⟨https://www.who.int/news-room/commentaries/detail/transmission-of-sars-cov-2-implications-for-infection-prevention-precautions⟩.
World Health Organization. Coronavirus disease (COVID-2019) situation reports. ⟨https://www.who.int/emergencies/diseases/novel-coronavirus-2019/situation-reports/⟩.
World Health Organization, 2014. Infection prevention and control of epidemic-and pandemic-prone acute respiratory infections in health care. ⟨https://apps.who.int/iris/bitstream/handle/10665/112656/9789241507134_eng.pdf;jsessionid=41AA684FB64571CE8D8A453C4F2B2096?sequence=1⟩.
Yin, Y., Xu, W., Gupta, J.K., Guity, A., Marmion, P., Manning, A., Gulick, B., Zhang, X., Chen, Q., 2009. Experimental study on displacement and mixing ventilation systems for a patient ward. HVACR Res. 15 (6), 1175–1191.
Yu, I.T., Li, Y., Wong, T.W., Tam, W., Chan, A.T., Lee, J.H., Ho, T., 2004. Evidence of airborne transmission of the severe acute respiratory syndrome virus. New Engl. J. Med. 350 (17), 1731–1739.
Zhang, Z., Chen, Q., 2007. Comparison of the Eulerian and Lagrangian methods for predicting particle transport in enclosed spaces. Atmos. Environ. 41 (25), 5236–5248.
Zhang, Z., Zhang, W., Zhai, Z.J., Chen, Q.Y., 2007. Evaluation of various turbulence models in predicting airflow and turbulence in enclosed environments by CFD: Part 2—Comparison with experimental data from literature. HvacR Res. 13 (6), 871–886.
Zhao, B., Zhang, Z., Li, X., 2005. Numerical study of the transport of droplets or particles generated by respiratory system indoors. Build. Environ. 40 (8), 1032–1039.
Zhou, L., Yao, M., Zhang, X., Hu, B., Li, X., Chen, H., Zhang, Y., 2021. Breath-, air-and surface-borne SARS-CoV-2 in hospitals. J. Aerosol Sci. 152, 105693.
Zhou, Y., Ji, S., 2021. Experimental and numerical study on the transport of droplet aerosols generated by occupants in a fever clinic. Build. Environ. 187, 107402.